The Canadian Mineralogist
Vol. 38, pp. 611-616 (2000)

THE CRYSTAL STRUCTURE OF $Cu_{1.6}Pb_{1.6}Bi_{6.4}S_{12}$, A NEW 44.8 Å DERIVATIVE OF THE BISMUTHINITE–AIKINITE SOLID-SOLUTION SERIES

DAN TOPA*, TONČI BALIĆ-ŽUNIĆ AND EMIL MAKOVICKY§

Geological Institute, University of Copenhagen, Øster Voldgade 10, DK-1350 Copenhagen K, Denmark

ABSTRACT

The crystal structure of $Cu_{1.60}Pb_{1.62}Bi_{6.38}S_{11.97}$, idealized $Cu_{1.6}Pb_{1.6}Bi_{6.4}S_{12}$, a new derivative of the aikinite–bismuthinite series from the metamorphosed scheelite deposit of Felbertal, Austria, with *a* 4.0074(9), *b* 44.81(1), *c* 11.513(3) Å, space group $Pmc2_1$, $Z = 4$, has been solved by direct methods and difference Fourier syntheses to a residual *R* value of ~4.7%. The unit cell of this "four-fold derivative" contains two "bismuthinite-like" Bi_2S_3 ribbons and six "krupkaite-like" $CuPbBi_3S_6$ ribbons. The fully occupied Cu sites occur in zigzag [001] rows $\Delta y \approx 0.25$ apart; the third [001] row, in which the Cu sites are 71% occupied, is $\Delta y \approx 0.375$ apart from them. The latter interval hosts a strongly zigzag pattern of 10% occupied Cu sites. Coordination polyhedra have been analyzed using the polyhedron-distortion parameters devised recently by Balić-Žunić & Makovicky. $Cu_{1.6}Pb_{1.6}Bi_{6.4}S_{12}$ occurs at Felbertal both as independent grains and as a component of exsolution pairs.

Keywords: $Cu_{1.6}Pb_{1.6}Bi_{6.4}S_{12}$, aikinite–bismuthinite derivative, crystal structure, Felbertal, scheelite deposit, Austria.

SOMMAIRE

Nous avons résolu la structure cristalline de $Cu_{1.60}Pb_{1.62}Bi_{6.38}S_{11.97}$, membre récemment reconnu de la série aikinite–bismuthinite dont la formule idéale serait $Cu_{1.6}Pb_{1.6}Bi_{6.4}S_{12}$, découvert dans le gisement de scheelite métamorphisé de Felbertal, en Autriche [*a* 4.0074(9), *b* 44.81(1), *c* 11.513(3) Å, groupe spatial $Pmc2_1$, $Z = 4$] par méthodes directes et synthèse de Fourier par différence, jusqu'à un résidu *R* d'environ 4.7%. La maille élémentaire de ce dérivé quadruple contient deux rubans Bi_2S_3 à caractère de bismuthinite, et six rubans $CuPbBi_3S_6$ à caractère de krupkaïte. Les sites Cu qui sont remplis sont distribués en zigzag en rangées le long de [001], séparées par Δy d'environ 0.25; la troisième rangée [001], dans laquelle les sites Cu sont occupés à 71%, est situé à $\Delta y \approx 0.375$ de ces dernières. Dans cet intervalle se trouve une rangée en zigzag plus frappant dont le taux d'occupation est 10%. Les polyèdres de coordinence ont été analysés selon les paramètres de distorsion proposés récemment par Balić-Žunić et Makovicky. A Felbertal, on trouve l'espèce $Cu_{1.6}Pb_{1.6}Bi_{6.4}S_{12}$ en grains indépendants et comme composant d'une texture d'exsolution.

(Traduit par la Rédaction)

Mots-clés: $Cu_{1.6}Pb_{1.6}Bi_{6.4}S_{12}$, dérivé d'aikinite–bismuthinite, structure cristalline, Felbertal, gisement de scheelite, Autriche.

INTRODUCTION

After the classical works of Ohmasa & Nowacki (1970a), Kohatsu & Wuensch (1976), Syneček & Hybler (1975), Mumme & Watts (1976), Mumme *et al.* (1976), and Žák (1980), the treatment of the ordered derivatives of the bismuthinite–aikinite solid-solution series $Cu_xPb_xBi_{2-x}S_3$ ($0 \le x \le 1$) appeared to be complete. Attention shifted to the composition ranges of these ordered structures (*e.g.*, Harris & Chen 1976, Makovicky & Makovicky 1978, Pring 1989, Mozgova *et al.* 1990). Syntheses of disordered intermediate compositions (Springer 1971, Mumme & Watts 1976) were followed by some annealing experiments to achieve order (Pring 1995).

Makovicky & Makovicky (1978) proposed to characterize these structures as members of the solid-solution series aikinite (x) – bismuthinite (100–x) or, in a short form, by n_a corresponding to the percentage of the $CuPbBiS_3$ end-member in the Bi_2S_3–$CuPbBiS_3$ series. The generally accepted picture is that of three compositions, Bi_2S_3 ($n_a = 0$, bismuthinite), $Cu_{0.5}Pb_{0.5}Bi_{1.5}S_3$ ($n_a = 50$, krupkaite), $CuPbBiS_3$ ($n_a = 100$, aikinite), which have simple orthorhombic structures with "11 × 11 × 4 Å unit cells" and only one type of structural ribbons (Bi_4S_6, $CuPbBi_3S_6$ and $Cu_2Pb_2Bi_2S_6$, respectively) in each structure. These three compositions are interleaved by additional ordered structures in which ribbons of two different types combine: $CuPbBi_{11}S_{18}$

* on leave from the Mineralogical Institute, University of Salzburg, Austria.
§ *E-mail address*: emilm@geo.geol.ku.dk

(n_a = 16.67), $CuPbBi_5S_9$ (n_a = 33.33), $Cu_2Pb_2Bi_4S_9$ (n_a = 66.67), $Cu_5Pb_5Bi_7S_{18}$ (n_a = 83.33), all these being of "33 × 11 × 4 Å type", and $Cu_3Pb_3Bi_7S_{15}$ (n_a = 80.0), the only phase of the "56 × 11 × 4 Å type".

New material from the metamorphosed scheelite deposit of Felbertal, Austria (Thalhammer *et al.* 1989), has altered substantially this well-established scheme. The deposit has yielded, in the form of independent grains and as lamellae in exsolution pairs, two phases of a new, "44 × 11 × 4 Å type", with compositions n_a = 40 and n_a = 67. The present communication concerns the crystal-structure determination of the first of these two phases, $Cu_{1.6}Pb_{1.6}Bi_{6.4}S_{12}$. The mineralogy for this deposit is currently the object of further investigation.

Experimental

The chemical composition of the analyzed crystal was obtained by electron-microprobe analysis before its extraction from a polished section. We used a JEOL–8600 electron microprobe equipped with Link EXL software with on-line ZAF correction. Analytical conditions employed were 25 kV and 30 nA; synthetic and natural sulfide standards were used. The analytical results (wt.%) are Cu 4.65, Fe 0.05, Pb 15.97, Bi 61.58, S 17.79, total 100.04. The resulting empirical formula is $Cu_{1.60}Pb_{1.64}Bi_{6.38}S_{11.97}$, *i.e.*, n_a = 40.5 or, alternatively, the mol% of the krupkaite end-member is equal to 81.0%, and that of the bismuthinite end-member, 19.0%.

A crystal with irregular shape and 0.04–0.09 mm diameter was measured on a Bruker AXS four-circle diffractometer equipped with CCD 1000K area detector (6.25 cm × 6.25 cm active detection-area, 512 × 512 pixels) and a flat graphite monochromator using Mo$K\alpha$ radiation from a fine-focus sealed X-ray tube. The sample – detector distance was fixed at 6 cm. In all, 1800 static exposures 0.3° apart were made, each measurement taking 90 s, with 94.7% coverage and average redundancy of 6.6 inside the limits of the angular span covered. The maximum 2θ value covered in the equatorial plane of detector was 56° (d = 0.76 Å) and Miller index limits were $4 \le h \le 5$, $55 \le k \le 54$, $13 \le l \le 13$. The SMART system of programs was used for unit-cell determination and data collection (Table 1), SAINT+ for the calculation of integrated intensities, and SHELXTL for the structure solution and refinement (all Bruker AXS products). For the empirical absorption correction, based on reflection measurements at different azimuthal angles and measurements of equivalent reflections, program XPREP from the SHELXTL package was used, and yielded a merging R_{INT} factor (for equivalents) of 0.0633 compared to 0.1348 before absorption correction. Minimum and maximum transmission-factors were 0.008 and 0.032, respectively. The systematic absences ($h0l$, $l = 2n + 1$, and $00l$, $l = 2n + 1$) are consistent with space groups $Pmc2_1$ and $Pmcm$. The former was chosen as consistent with structures of the bismuthinite–aikinite family. The structure was solved by direct methods, which suggested a solution revealing the positions of Bi and Pb atoms together with three principal Cu sites and most of the S atoms. In subsequent refinements, the positions of the remaining S atoms and two Cu sites with lower occupancies were deduced from the difference-Fourier syntheses.

An additional check of the Cu distribution was made by lowering the symmetry to Pm, which makes all of the theoretically possible 16 Cu positions in the unit cell unique. The difference-Fourier map was then calculated with only one Cu position occupied to fix the origin. The additional Cu positions that appeared in the map and that could subsequently be refined conformed to the distribution found in the $Pmc2_1$ model, with positions corresponding to Cu2 and Cu3 showing practically full occupancy, and positions corresponding to Cu1 having somewhat lower occupancy. The low maxima appeared also at positions corresponding to Cu4 and Cu5, which were refined with *ca.* 10% occupancy in $Pmc2_1$.

After the final refinement in $Pmc2_1$, with anisotropic temperature-factors used for all the atoms except Cu4 and Cu5, for which they were fixed to isotropic values of 0.03 (about the average for S atoms), the highest residual peak was 4 e/Å^3, 0.86 Å from Pb1 and the deepest hole –3 e/Å^3, 0.87 Å from the same atom. The refinement was stopped when the maximum shift/e.s.d. for varied parameters dropped below 1. The results of the refinement are represented in Table 2 and Figure 1, interatomic distances in Table 3 (deposited). Structure factors may be obtained from the Depository of Unpublished Data, CISTI, National Research Council, Ottawa, Ontario K1A 0S2, Canada.

Description of the structure

The crystal structures of bismuthinite–aikinite series are superstructures of the Bi_2S_3 structure, with *en échelon* Me_4S_6 ribbons (*Me* = Bi, Pb). The adjacent tetrahedral voids are capable of accommodating Cu atoms. For each occupied Cu site, the inner Bi position in the adjacent Bi_4S_6 ribbon is replaced by Pb.

The unit cell of $Cu_{1.6}Pb_{1.6}Bi_{6.4}S_{12}$, a unidimensional quadruple of the unit cell of Bi_2S_3, contains eight Me_4S_6

TABLE 1. CRYSTAL DATA AND STRUCTURE-REFINEMENT INFORMATION FOR $Cu_{1.6}Pb_{1.6}Bi_{6.4}S_{12}$

measured reflections: 12598	unique: 3717 (2745 with $I > 2\sigma_I$)
temperature: 299 K	space group: $Pmc2_1$
lattice parameters: a 4.0074(9), b 44.81(1), c 11.513(3) Å,	V 2068(1) Å^3
(refined from 3156 reflections with $I > 10\sigma_I$)	
$Z = 4$	ρ_c = 6.904 g/cm^3 μ = 69.98 mm^{-1}
full-matrix refinement	
weighting scheme: $1/\{\sigma^2_{Fo}{}^2 + [0.0747(\mathrm{Max}(F_o^2,0) + 2F_c^2)/3]\}$	
(giving a flat analysis of variance in terms of F_c^2)	
R factors: $\{\Sigma[\omega(F_O^2 - F_C^2)^2]/\Sigma[\omega(F_O^2)^2]\}^2$ = 0.1381;	
$\Sigma\omega\|\|F_C\| - \|F_O\|\|/\Sigma\omega\|F_O\|$ = 0.0467 (for $F_o > 4\sigma_{Fo}$), 0.0641 (for all)	
scale factor: 0.03228	

TABLE 2. ATOMIC PARAMETERS FOR $Cu_{1.6}Pb_{1.6}Bi_{6.4}S_{12}$

Atom	*x*	*y*	*z*	sof	U11	U22	U33	U23	Ueq
Pb1	0.0	0.06361 (6)	0.7982 (3)	1.00	0.037 (1)	0.039 (1)	0.025 (2)	−0.004 (1)	0.0335 (6)
Pb2	0.5	0.31075 (5)	0.1624 (3)	1.00	0.038 (1)	0.032 (1)	0.051 (2)	−0.009 (1)	0.0404 (7)
Pb3	0.5	0.43703 (6)	0.6634 (3)	1.00	0.037 (1)	0.044 (1)	0.042 (2)	0.013 (1)	0.0406 (7)
Bi1	0.5	0.01584 (5)	0.4536 (2)	1.00	0.026 (1)	0.028 (1)	0.025 (2)	0.002 (1)	0.0264 (6)
Bi2	0.0	0.39060 (5)	0.0091 (2)	1.00	0.029 (1)	0.035 (1)	0.026 (2)	−0.001 (1)	0.0300 (6)
Bi3	0.0	0.35861 (5)	0.5042 (3)	1.00	0.028 (1)	0.036 (1)	0.031 (2)	0.007 (1)	0.0317 (6)
Bi4	0.0	0.14475 (5)	−0.0009 (2)	1.00	0.026 (1)	0.026 (1)	0.028 (2)	−0.004 (1)	0.0265 (6)
Bi5	0.5	0.22969 (5)	0.9590 (3)	1.00	0.028 (1)	0.025 (1)	0.031 (2)	−0.004 (1)	0.0279 (6)
Bi6	0.5	0.48024 (5)	0.9714 (3)	1.00	0.028 (1)	0.030 (1)	0.036 (2)	−0.000 (1)	0.0312 (7)
Bi7	0.5	0.07147 (5)	0.1293 (2)	1.00	0.032 (1)	0.033 (1)	0.029 (2)	0.005 (1)	0.0314 (7)
Bi8	0.0	0.30362 (5)	0.8318 (2)	1.00	0.034 (1)	0.027 (1)	0.044 (2)	−0.008 (1)	0.0349 (6)
Bi9	0.0	0.44720 (5)	0.3349 (2)	1.00	0.036 (1)	0.030 (1)	0.025 (2)	−0.009 (1)	0.0303 (7)
Bi10	0.0	0.10636 (5)	0.4879 (2)	1.00	0.027 (1)	0.027 (1)	0.023 (2)	0.003 (1)	0.0260 (6)
Bi11	0.5	0.26746 (5)	0.4706 (3)	1.00	0.027 (1)	0.030 (1)	0.036 (2)	0.004 (1)	0.0310 (7)
Bi12	0.5	0.17756 (5)	0.6374 (2)	1.00	0.030 (1)	0.028 (1)	0.033 (2)	0.002 (1)	0.0303 (6)
Bi13	0.0	0.19673 (5)	0.3208 (2)	1.00	0.032 (1)	0.043 (1)	0.033 (2)	0.008 (1)	0.0358 (6)
Cu1	0.0	0.00907 (15)	0.2004 (9)	0.71 (2)	0.023 (5)	0.011 (4)	0.017 (5)	0.003 (3)	0.0170 (29)
Cu2	0.5	0.38377 (16)	0.2609 (8)	0.99 (2)	0.040 (4)	0.042 (4)	0.026 (4)	0.001 (3)	0.0362 (25)
Cu3	0.5	0.36506 (14)	−0.2392 (6)	0.97 (2)	0.036 (4)	0.039 (4)	0.022 (4)	0.003 (3)	0.0325 (24)
Cu4	0.5	0.13758 (129)	0.2360 (53)	0.10 (1)	0.030				
Cu5	0.0	0.23871 (143)	0.7081 (66)	0.10 (2)	0.030				
S1	0.0	0.04743 (28)	0.3507 (15)	1.00	0.036 (8)	0.021 (6)	0.024 (8)	0.003 (6)	0.0266 (31)
S2	0.0	0.03126 (29)	0.0171 (14)	1.00	0.021 (7)	0.035 (7)	0.020 (8)	0.014 (6)	0.0254 (31)
S3	0.0	0.11069 (26)	0.1938 (13)	1.00	0.035 (8)	0.012 (5)	0.014 (8)	0.007 (5)	0.0206 (31)
S4	0.5	0.17390 (34)	0.1049 (16)	1.00	0.016 (7)	0.043 (8)	0.040 (9)	0.011 (7)	0.0328 (36)
S5	0.5	0.09749 (30)	0.9309 (15)	1.00	0.018 (7)	0.031 (7)	0.033 (10)	−0.015 (7)	0.0274 (34)
S6	0.5	0.01444 (29)	0.7576 (15)	1.00	0.024 (7)	0.025 (6)	0.020 (8)	−0.001 (6)	0.0228 (31)
S7	0.5	0.42267 (27)	0.1144 (15)	1.00	0.030 (8)	0.023 (6)	0.022 (8)	0.010 (6)	0.0248 (31)
S8	0.5	0.34362 (28)	0.9438 (13)	1.00	0.030 (8)	0.025 (6)	0.022 (8)	−0.009 (6)	0.0258 (31)
S9	0.5	0.26440 (31)	0.7674 (15)	1.00	0.025 (8)	0.028 (7)	0.027 (9)	−0.007 (6)	0.0266 (34)
S10	0.0	0.20123 (29)	0.8531 (13)	1.00	0.039 (8)	0.026 (6)	0.012 (7)	−0.011 (6)	0.0255 (31)
S11	0.0	0.27640 (27)	0.0328 (13)	1.00	0.032 (7)	0.022 (6)	0.022 (8)	0.006 (6)	0.0254 (31)
S12	0.0	0.36002 (33)	0.2060 (17)	1.00	0.031 (9)	0.028 (7)	0.041 (11)	0.008 (7)	0.0333 (38)
S13	0.5	0.32776 (28)	0.6075 (15)	1.00	0.022 (7)	0.023 (6)	0.030 (8)	0.001 (6)	0.0249 (30)
S14	0.5	0.40576 (27)	0.4409 (13)	1.00	0.034 (8)	0.024 (6)	0.015 (8)	0.008 (6)	0.0245 (32)
S15	0.5	0.48695 (28)	0.2753 (14)	1.00	0.028 (7)	0.022 (6)	0.019 (8)	0.007 (6)	0.0231 (31)
S16	0.0	0.45007 (28)	0.8685 (13)	1.00	0.050 (9)	0.018 (6)	0.014 (7)	−0.012 (5)	0.0272 (34)
S17	0.0	0.47274 (30)	0.5386 (14)	1.00	0.042 (9)	0.030 (7)	0.016 (8)	−0.007 (6)	0.0293 (34)
S18	0.0	0.38868 (27)	0.7039 (15)	1.00	0.040 (9)	0.011 (5)	0.032 (9)	−0.008 (6)	0.0280 (35)
S19	0.5	0.07648 (29)	0.5895 (13)	1.00	0.013 (6)	0.029 (6)	0.024 (8)	0.002 (5)	0.0219 (31)
S20	0.5	0.15537 (28)	0.4278 (14)	1.00	0.016 (7)	0.024 (6)	0.027 (8)	0.000 (6)	0.0226 (30)
S21	0.5	0.23728 (28)	0.2720 (13)	1.00	0.017 (6)	0.022 (6)	0.020 (8)	0.005 (6)	0.0196 (29)
S22	0.0	0.29897 (32)	0.3714 (15)	1.00	0.059 (11)	0.025 (7)	0.023 (9)	−0.002 (6)	0.0359 (39)
S23	0.0	0.21847 (28)	0.5290 (14)	1.00	0.036 (8)	0.018 (6)	0.025 (8)	−0.006 (6)	0.0262 (32)
S24	0.0	0.13694 (28)	0.6902 (15)	1.00	0.027 (8)	0.020 (6)	0.033 (10)	−0.007 (6)	0.0267 (34)

U12 = U13 = 0.

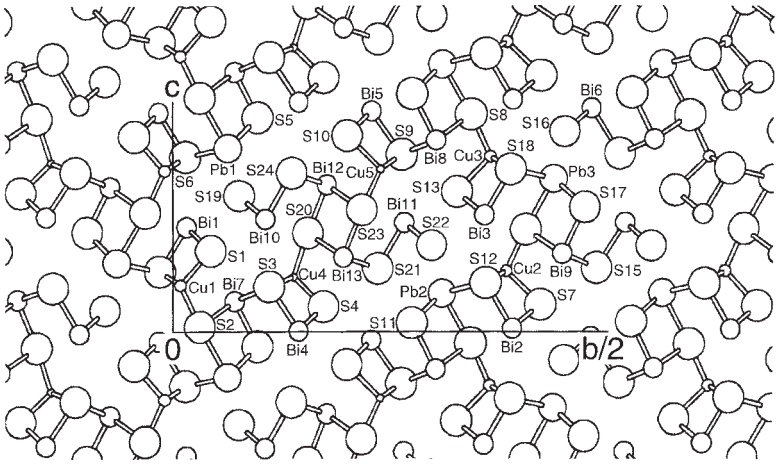

FIG. 1. Atom labeling in the crystal structure of $Cu_{1.6}Pb_{1.6}Bi_{6.4}S_{12}$.

ribbons in an *n*-glide-related herringbone arrangement (Fig. 2). Ignoring the presence of two 10%-occupied tetrahedral sites, it contains two Bi_4S_6 "bismuthinite-like" ribbons and six $CuPbBi_3S_6$ "krupkaite-like" ribbons. In each [010] row, two of the latter ribbons are oriented in one way and one in the opposite way.

The fully occupied Cu sites Cu2 and Cu3 occur in two zigzag [001] rows $\Delta y \approx 0.25$ apart, at $y \approx 0.375$ and ≈ 0.625 (Fig. 1). The third [001] row of occupied Cu sites (Cu1 with 71% occupancy) is based on a 2_1 axis at $y \approx 0$, *i.e.*, $\Delta y \approx 0.375$ from the previous rows. Adjacent Cu2 – Cu3 rows are separated by a single row of unoccupied Cu sites situated along the 2_1 axis at $y = 0.5$. The Cu2 – Cu3 rows are separated from the Cu1 rows by two zigzag [001] rows of potential Cu sites (Fig. 2). These broader intervals are occupied by a statistical distribution of Cu4 and Cu5 (~10% occupancy), in a strongly zigzag pattern stretching over two adjacent, sparsely occupied [001] rows of tetrahedra. This distribution of Cu atoms preserves the pure "bismuthinite-like" Bi_4S_6 character of ribbons, above and below which Cu4 and Cu5 occur. It also speaks against the possibility of being produced as a result of stacking errors in the width of interspaces between the consecutive [001] rows of (nearly) fully occupied Cu sites.

The fully occupied Cu2–Cu3 sites have a slightly eccentric coordination typical for the bismuthinite–aikinite derivatives (*e.g.*, Kohatsu & Wuensch 1976). The 70% occupied Cu1 position approaches this situation as well (Table 3). The 10% occupied sites have apparently more distorted bond-lengths because the proportion of S positions related to unoccupied tetrahedra to those related to Cu-occupied tetrahedra in the same site is 9:1.

The Pb1, 2 and 3 sites, related spatially to Cu1–3, have typical lead–sulfur bonds. The partly lead-occupied sites Bi7 and 8 adjacent to the sparsely occupied Cu4 and Cu5 sites do not show visible deviations from the remaining Bi sites.

TABLE 4. POLYHEDRON DISTORTION-PARAMETERS FOR CATIONS IN $Cu_{1.6}Pb_{1.6}Bi_{6.4}S_{12}$

Atom	CN	Sphere radius, std. deviation	Sphere volume	Polyhedron volume	Volume distortion[1]	Eccentricity [2]	Sphericity [3]
Pb1	7	3.026 ± 0.113	116.962	38.386	0.1327	0.1630	0.9779
Pb2	7	3.026 ± 0.111	116.652	38.376	0.1306	0.1589	0.9767
Pb3	7	3.011 ± 0.100	114.975	38.080	0.1248	0.1436	0.9710
Bi1	7	2.960 ± 0.301	109.340	37.216	0.1005	0.3988	0.9485
Bi2	7	2.969 ± 0.295	110.016	37.474	0.0999	0.3883	0.9384
Bi3	7	2.943 ± 0.275	107.283	36.661	0.0969	0.3699	0.9503
Bi4	7	2.961 ± 0.317	108.701	36.776	0.1060	0.4072	0.9050
Bi5	7	2.959 ± 0.337	108.109	36.573	0.1060	0.4264	0.8886
Bi6	7	2.952 ± 0.298	107.770	36.622	0.1020	0.3917	0.9235
Bi7	7	2.987 ± 0.327	113.089	37.220	0.1303	0.4499	0.9503
Bi8	7	3.000 ± 0.329	114.503	37.681	0.1304	0.4441	0.9286
Bi9	7	2.994 ± 0.318	113.429	37.623	0.1235	0.4328	0.9390
Bi10	7	2.948 ± 0.271	107.703	36.689	0.0998	0.3657	0.9593
Bi11	7	2.958 ± 0.282	109.079	37.169	0.0995	0.3804	0.9699
Bi12	7	2.980 ± 0.292	112.149	37.136	0.1250	0.4099	0.9582
Bi13	7	2.973 ± 0.296	111.498	36.847	0.1267	0.4163	0.9649
Cu1	4	2.372 ± 0.046	55.378	6.593	0.0283	0.0907	1.0000
Cu2	4	2.358 ± 0.054	54.405	6.516	0.0225	0.1013	1.0000
Cu3	4	2.366 ± 0.048	54.978	6.532	0.0302	0.0911	1.0000
Cu4	4	2.336 ± 0.080	53.821	6.466	0.0195	0.1563	1.0000
Cu5	4	2.360 ± 0.074	54.806	6.545	0.0253	0.1296	1.0000

The centroid parameters used are defined in Balić-Žunić & Makovicky (1996) and Makovicky & Balić-Žunić (1998). The volume distortions are calculated using the maximum volume polyhedra for respective CN (7 = regular pentagonal bipyramid, 4 = regular tetrahedron) as ideal reference.

(1) Volume distortion $\upsilon = [V(\text{ideal}) - V(\text{polyhedron})]/V(\text{ideal})$ to be multiplied by 100 to obtain percentage.

(2) "Volume-based" eccentricity $ECC_V = 1 - [(r_s - \Delta)/r_s]^3$, where r_s is the radius of the circumscribed sphere and Δ is the distance between the sphere center ('centroid') and the central atom.

(3) "Volume-based" sphericity $SPH_V = 1 - 3\sigma_r/r_s$, where σ_r is a standard deviation of the radius r_s.

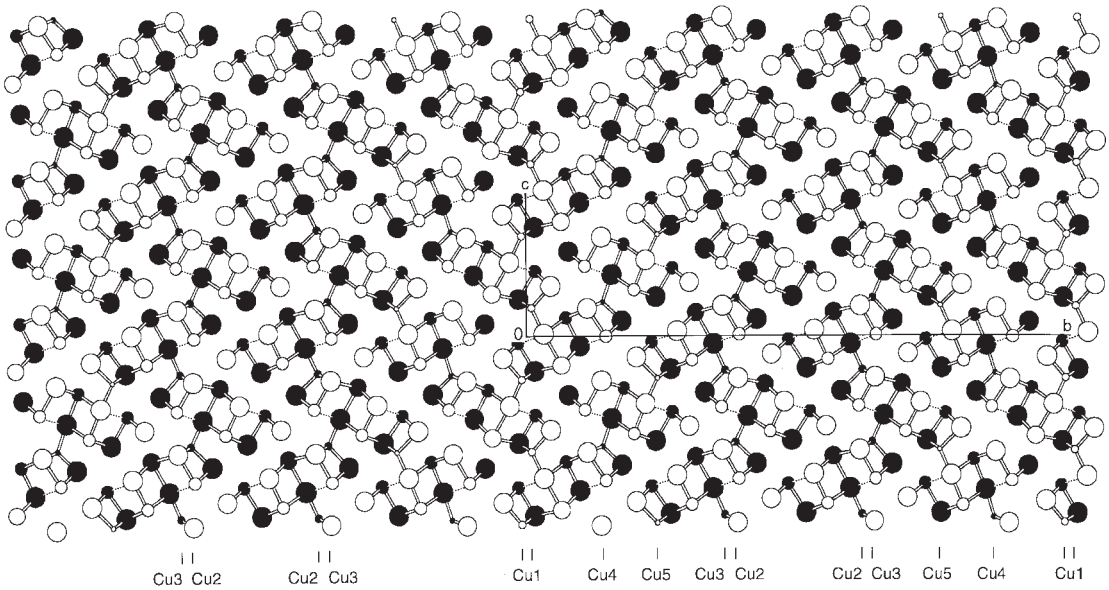

FIG. 2. The crystal structure of $Cu_{1.6}Pb_{1.6}Bi_{6.4}S_{12}$. In order of increasing size, circles represent partly and fully occupied Cu positions, (predominantly) Bi sites, Pb and S. Void and filled circles represent atoms at two *x* levels, 2 Å apart. Selected [001] rows of Cu atoms are indicated.

Polyhedron-distortion parameters

In the process of characterization of polyhedron distortion (Balić-Žunić & Makovicky 1996, Makovicky & Balić-Žunić 1998), a least-squares-fitted sphere is circumscribed to the coordination polyhedron. Its volume is compared to that of the polyhedron and to the volume of an ideal polyhedron with the same coordination number (CN), which is inscribed in the same sphere as the observed polyhedron. This comparison (Table 3) yields a measure of polyhedron distortion. "Sphericity" is a measure of the fit of ligands to the sphere, and "eccentricity" expresses a displacement of the cation from the center of the sphere (Table 4). All calculations have been performed with CN = 7 for the large cations and CN = 4 for copper. The central cations of the Me_4S_6 ribbons (*i.e.*, Pb1–3, Bi7–9, 12 and 13) have minimal polyhedron distortions when compared with the ideal "split octahedron" (monocapped trigonal prism with cation in the capped wall and seven equal cation–ligand distances). The "apical" anions (*i.e.*, the remaining Bi atoms) deviate more from this model, by several percent toward the V_s/V_p ratio typical of the pentagonal bipyramid (Makovicky & Balić-Žunić 1998).

The measure of distortion for the ideal split octahedron, when its polyhedron volume is taken as V_r and compared to that of the pentagonal prism taken as V_i, is equal to 0.1333. This value should be compared with the ν values calculated for the observed polyhedra in Table 4. The universal trend, albeit quantitatively different for the two coordination types, toward the volumetrically "more efficient" coordination is caused by the fact that in the ideal "split octahedron", all bond lengths are equal, distorting the shape of its trigonal–prismatic part, whereas in the present structure the cation–ligand distances across the prism space are longest of all, and the "prism flattening" just mentioned is limited or it does not take place. The larger deviation of the "apical" Bi atoms from the split octahedron model indicates that their lone pairs of electrons have steric activities higher than those of the "central" cations. The principal difference between the Pb and Bi polyhedra comprises (a) larger polyhedral and sphere volumes for Pb, (b) much larger eccentricity of Bi (demonstrating its active lone pairs of electrons), and (c) consistently lower sphericities for the latter element.

The polyhedron volume and the fairly variable sphericity of Bi do not seem to depend on its position in the ribbons. However, the "central" Bi atoms have somewhat larger volumes of circumscribed spheres and higher eccentricities when compared to the "apical" ones, in agreement with the conclusions reached from the differences in their distortion coefficients.

With the possible exception of Cu4, the volumes of circumscribed spheres and the polyhedron volumes for the coordination tetrahedra of copper do not depend on the Cu-occupancy factors (Table 4). However, the eccentricity of the weakly occupied Cu sites is appreciably larger than the eccentricity of the (nearly) fully occupied sites Cu1 – Cu3, which show values characteristic for other aikinite–bismuthite derivatives.

TABLE 5. POLYHEDRON DISTORTION-PARAMETERS FOR CATIONS IN Bi_2S_3 AND $CuPbBiS_3$

Atom[1]	CN	Sphere radius, std. deviation	Sphere volume	Polyhedron volume	Volume[2] distortion	Eccentricity[2]	Sphericity[2]
Bi1 (b)	7	2.932 ± 0.033	105.574	35.906	0.1012	0.3592	0.9659
Bi2 (b)	7	2.947 ± 0.032	107.203	35.463	0.1258	0.4059	0.9675
Bi1 (a)	7	2.968 ± 0.080	109.546	37.179	0.1031	0.3891	0.9193
Pb1 (a)	7	3.061 ± 0.035	120.167	40.023	0.1199	0.2108	0.9657
Cu1 (a)	4	2.350 ± 0.0	54.389	6.504	0.0240	0.0707	1.000

(1) Cations in bismuthinite Bi_2S_3 (Kupčík & Veselá-Nováková 1970) are denoted by (b), those in aikinite $CuPbBiS_3$ (Ohmasa & Nowacki 1970b), by (a).
(2) Definitions are given in the footnotes to Table 4.

Comparison of the distortion parameters for $Cu_{1.6}Pb_{1.6}Bi_{6.4}S_{12}$ with such parameters for the corresponding positions in Bi_2S_3 (bismuthinite) and $CuPbBiS_3$ (aikinite) (Table 5) corroborates the high degree of polyhedral and modular unity in the structures of the bismuthinite–aikinite series. All tenets postulated for the present structure are valid for the end-members as well. This comparison also reveals the distribution of the increase in the unit-cell volume that takes place from Bi_2S_3 to $CuPbBiS_3$, among the individual cation polyhedra.

Epilogue

The exceptional geological conditions at Felbertal, Austria, led to the formation and preservation of aikinite–bismuthite derivatives with ordering periodicities equal to four-fold multiples of the substructure motif. This discovery leads to a revision of models for the mechanisms of cation ordering in this series and of the tentative composition – temperature diagram Bi_2S_3 – $CuPbBi_3S_6$. In addition to the present structural investigations, the voluminous compositional and textural data obtained from that locality will be used in this revision.

Acknowledgements

This research was supported by a grant to D. Topa from the University of Salzburg, Austria. The diffraction equipment was financed by the Danish Natural Science Research Council. Active interest and support of Prof. W. Paar (Salzburg), professional assistance of Mrs. Britta Munch and Mrs. Camilla Sarantaris as well as the helpful suggestions by Drs. A. Pring, N.I. Organova and the editor, R.F. Martin, are gratefully acknowledged.

References

Balić-Žunić, T. & Makovicky, E. (1996): Determination of the centroid or 'the best centre' of a coordination polyhedron. *Acta Crystallogr.* **B52**, 78-81.

Harris, D.C. & Chen, T.T. (1976): Crystal chemistry and re-examination of nomenclature of sulfosalts in the aikinite–bismuthinite series. *Can. Mineral.* **14**, 194-205.

Kohatsu, I. & Wuensch, B.J. (1976): The crystal structure of gladite, $PbCuBi_5S_9$, a superstructure intermediate in the series Bi_2S_3–$PbCuBiS_3$ (bismuthinite – aikinite). *Acta Crystallogr.* **B32**, 2401-2409.

Kupčík, V. & Veselá-Nováková, L. (1970): Zur Kristallstruktur des Bismuthinits, Bi_2S_3. *Tschermaks Mineral. Petrogr. Mitt.* **14**, 55-59.

Makovicky, E. & Balić-Žunić, T. (1998): New measure of distortion for coordination polyhedra. *Acta Crystallogr.* **B54**, 766-773.

_____ & Makovicky, M. (1978): Representation of compositions in the bismuthinite–aikinite series. *Can. Mineral.* **16**, 405-409.

Mozgova, N.N., Nenasheva, S.N., Chistyakova, N.I., Mogilevkin, S.B. & Sivtsov, A.V. (1990): Compositional fields of minerals in the bismuthinite–aikinite series. *Neues Jahrb. Mineral., Monatsh.*, 35-45.

Mumme, W.G. & Watts, J.A. (1976): Pekoite, $CuPbBi_{11}S_{18}$, a new member of the bismuthinite–aikinite mineral series: its crystal structure and relationship with naturally- and synthetically-formed members. *Can. Mineral.* **14**, 322-333.

_____, Welin, E. & Wuensch, B.J. (1976): Crystal chemistry and proposed nomenclature for sulfosalts intermediate in the system bismuthinite–aikinite (Bi_2S_3–$CuPbBiS_3$). *Am. Mineral.* **61**, 15-20.

Ohmasa, M. & Nowacki, W. (1970a): Note on the space group and on the structure of aikinite derivatives. *Neues Jahrb. Mineral., Monatsh.*, 158-162.

_____ & _____ (1970b): A redetermination of the crystal structure of aikinite [$BiS_2|S|Cu^{IV}Pb^{VII}$]. *Z. Kristallogr.* **132**, 71-86.

Pring, A. (1989): Structural disorder in aikinite and krupkaite. *Am. Mineral.* **74**, 250-255.

_____ (1995): Annealing of synthetic hammarite, $Cu_2Pb_2Bi_4S_9$, and the nature of cation-ordering processes in the bismuthinite–aikinite series. *Am. Mineral.* **80**, 1166-1173.

Springer, G. (1971): The synthetic solid-solution series Bi_2S_3–$BiCuPbS_3$ (bismuthinite–aikinite). *Neues Jahrb. Mineral., Monatsh.*, 19-24.

Syneček, V. & Hybler, J. (1975): The crystal structure of krupkaite, $CuPbBi_3S_6$, and of gladite, $CuPbBi_5S_9$, and the classification of superstructures in the bismuthinite–aikinite group. *Neues Jahrb. Mineral., Monatsh.*, 541-560.

Thalhammer, O.A.R., Stumpfl, E.F. & Jahoda, R. (1989): The Mittersill scheelite deposit, Austria. *Econ. Geol.* **84**, 1153-1171.

Žák, L. (1980): Isomorphism and polymorphism in the bismuthinite–aikinite group. *Neues Jahrb. Mineral., Monatsh.*, 440-448.

Received December 17, 1999, revised manuscript accepted March 29, 2000.